Fish & Shellfish Immunology 45 (2015) 367–377

Contents lists available at ScienceDirect

Fish & Shellfish Immunology

journal homepage: www.elsevier.com/locate/fsi

Full length article

High-throughput transcriptome analysis of ISAV-infected Atlantic salmon *Salmo salar* unravels divergent immune responses associated to head-kidney, liver and gills tissues

Diego Valenzuela-Miranda [a], Sebastian Boltaña [a], Maria E. Cabrejos [c], José M. Yáñez [b, d], Cristian Gallardo-Escárate [a, *]

[a] Laboratory of Biotechnology and Aquatic Genomics, Interdisciplinary Center for Aquaculture Research (INCAR), University of Concepción, P.O. Box 160-C, Concepción, Chile
[b] Aquainnovo, Talca 60, P.O. Box 30B, Puerto Montt 5503032, Chile
[c] Facultad de Ciencias Agronómicas, Universidad de Chile, Av Santa Rosa 11315, La Pintana, Santiago 8820808, Chile
[d] Facultad de Ciencias Veterinarias y Pecuarias, Universidad de Chile, Av Santa Rosa 11735, La Pintana, Santiago 8820808, Chile

ARTICLE INFO

Article history:
Received 15 September 2014
Received in revised form
2 April 2015
Accepted 4 April 2015
Available online 21 April 2015

Keywords:
RNA-seq
ISAV
Viral segments
rt-qPCR
Salmo salar

ABSTRACT

Infectious salmon anaemia virus (ISAV) is an orthomyxovirus causing high mortality in farmed Atlantic salmon (*Salmo salar*). The collective data from the Atlantic salmon–ISAV interactions, performed "in vitro" using various salmon cell lines and "*in vivo*" fish infected with different ISAV isolates, have shown a strong regulation of immune related transcripts during the infection. Despite this strong defence response, the majority of fish succumb to infections with ISAV. The deficient protection of the host against ISAV is in part due to virulence factors of the virus, which allow evade the host-defence machinery. As such, the viral replication is uninhibited and viral loads quickly spread to several tissues causing massive cellular damage before the host can develop an effective cell-mediated and humoral outcome. To interrogate the correlation of the viral replication with the host defence response, we used fish that have been infected by cohabitation with ISAV-injected salmons. Whole gene expression patterns were measured with RNA-seq using RNA extracted from Head-kidney, Liver and Gills. The results show divergent mRNA abundance of functional modules related to interferon pathway, adaptive/innate immune response and cellular proliferation/differentiation. Furthermore, gene regulation in distinct tissues during the infection process was independently controlled within the each tissue and the observed mRNA expression suggests high modulation of the ISAV-segment transcription. Importantly this is the first time that strong correlations between functional modules containing significant immune process with protein–protein affinities and viral-segment transcription have been made between different tissues of ISAV-infected fish.

1. Introduction

Infectious salmon anaemia virus (ISAV) has a genome of eight single-stranded RNA molecules of negative polarity and is the type virus of the genus Isavirus in the family Orthomyxoviridae [1–3]. It is the etiologic agent of infectious salmon anaemia (ISA) a disease that causes high mortality in aquaculture of Atlantic salmon (Salmo salar) [4–8]. The ISAV is principally spread through the cohabitation of infected and healthy fish [9,10], with the gills and heart acting as the main entry points of infection and with the kidney, liver, and spleen being the main tissues affected [11,12]. In addition to anaemia, macroscopic lesions during ISAV infection include petechial haemorrhaging of the skin, intestinal congestion, gill pallor, liver enlargement, and haemorrhagic kidney syndrome [13–15].

As is the case in most host–pathogen interactions, the perceived resistance of the host is highly dependent on the host immune competence to trigger an effective defence response against the pathogen. The collective data from the Atlantic salmon–ISAV interactions studies, performed in vitro using various salmonid cell

* Corresponding author.
E-mail address: crisgallardo@udec.cl (C. Gallardo-Escárate).

http://dx.doi.org/10.1016/j.fsi.2015.04.003
1050-4648/

lines [16–19] and *in vivo* in Atlantic salmon infected with different ISAV isolates [17,20–22], have shown a strong regulation of immune transcripts during the infection. Despite this immune response, the majority of fish fall upon some ISAV isolates. The lack protection of the host against ISAV is in part due to virulence factors in the virus, which allow evade the host defence machinery [23,24].

As such, the viral replication is uninhibited and viral loads quickly spread to several tissues causing massive cellular damage before the host can develop an effective cell-mediated and humoral defence response. The replication of ISAV take place in the nucleus of the infected cell [25,26], where the viral genomic, complementary and messenger RNAs are synthesized by the viral transcriptase complex. Like other orthomyxovirus ISAV mRNAs have capped, heterogeneous 5′-ends and their synthesis is inhibited by α-amanitin, a specific inhibitor of the cellular RNA polymerase II due to the need of capped host nuclear RNAs as primers for mRNA synthesis [25]. The nuclear replication requires nuclear export of viral mRNAs, and nuclear import of the viral proteins of the ribonucleoproteins (RNP), i.e. the nucleoprotein (NP) and the viral transcriptase complex, as well as of matrix protein (M), and finally nuclear export of the RNP–M complex. A miss understanding the mechanisms of viral replication in critical organs and its correlation with a tissue defence response is needed to the development of new and highly effective vaccines strategies.

Recently, Chilean ISAV reports have mainly been produced through the non-virulent HPR0 ISAV strain. However, the increasing prevalence of HPR0 ISAV has been suggested as a potential risk due to the capacity of HPR0 to mutate into a virulent strain [27]. Considering the latent threat to the salmonid aquaculture industry and the little information available on the molecular mechanisms that are regulated during the course of an ISAV infection, we explore novel insights of the transcriptome responses that have not been addressed yet by using microarray based approaches. To interrogate the correlation with the viral replication, we used fish that have been infected by cohabitation with intraperitoneal injected (trojan) fish of ISAV. Global gene expression patterns were evaluated from head-kidney, liver and gills tissues. The molecular results were analysed in more detail using statistical modelling of viral segments transcription (1–8) obtained from each tissue examined. In addition, the expression levels of the host transcriptomic response were also monitored and statistically analysed to determine if infection ISAV had variable effects on the immune system. Our results showed a correlation between mRNA abundance from specific viral segment and a tissue specific expression pattern, and suggest a strong response associated with innate/adaptive immune response, antiviral and cell activation/proliferation, as well as the involvement of a novel intracellular interferon related transcripts that are highly regulated during ISAV infection. Thus the results of this study contribute to a better understanding of the pathogenesis of this important pathogen in Atlantic salmon aquaculture, and how networks and intensity of regulation within gene regulatory networks i.e. connectivity appear to underlie the differences observed of the immune response in each tissue.

2. Materials and methods

2.1. Ethic statements

All animal procedures were carried out under the guidelines and approved by the ethics committee of University of Concepción and fulfilling the statements of the Animal Welfare Protocol (AWP) from Aquainnovo. All laboratory infections and cultures procedure were carried on under appropriate veterinary supervision, using tricaine anaesthetics to ameliorate animal suffering.

2.2. Experimental individuals

One thousand four hundred individuals of *Salmo salar* (108 ± 7.74 g, 22.3 ± 0.53 cm) were obtained from a commercial farm (Hornopirén, Puerto Montt, Chile) and transferred to the "Centro de Investigación y Transferencia Acuicola" (CITA) Aquainnovo S.A (Lenca, Puerto Montt, Chile). Individuals were sanitarily checked to discard the presence of *Piscirickettsia salmonis* bacteria (SRS), the infectious pancreatic necrosis virus (IPNV), and the infectious salmon anaemia virus (ISAV). Once completed, all individuals were acclimated for 26 days. After quarantine, 160 *S. salar* were randomly divided into four tanks (0.5 m^3) and maintained until the cohabitation challenge. One tank was used to determine mortality, and the remaining three were used for tissue sampling.

2.3. Cohabitation challenge

Cohabitant infection was chosen because it better imitates the natural route of infection. Just before the beginning of the challenge, head-kidney, liver and gills were sampled from eight randomly selected individuals, used as control group (T0). Then, for each tank, 12 fish (30%), henceforth called trojans, were Pit-tagged and received an intraperitoneal (IP) injection of 10^3 $TCID_{50}$ of the virulent HPR7b ISAV strain isolated by Novartis (NPV-090). The remaining 28 individuals (70%) were considered cohabitants and were used for tissue sampling. The infective dose of ISAV suitable for cohabitation and tank parameters had been determined in a pre-challenge trial using the same population density and water flow rate as in the experiment. The mortality produced by the ISAV infection was molecular and clinically confirmed, with an ISA outbreak declared after three consecutive days of dead trojans. Then, head-kidney, gills and liver were sampled from without visible symptoms 3 (T1), 7 (T2), and 14 (T3) days after the ISAV outbreak was declared, for a total of 4 sampled points (Fig. 1). Liver, head kidney and gills samples were taken. Samples were collected from eight fish before vaccination, and from eight fish of each group at 3 and 6 wpv but prior to challenge. After ISAV challenge, samples from eight fish of each group were taken at T0, T1 and T2. Eight individuals were randomly sampled per point, and tissues were stored in RNAlater® solution (Ambion, USA) at −80 °C until total RNA extraction. To verify that ISA was the cause of death, liver and

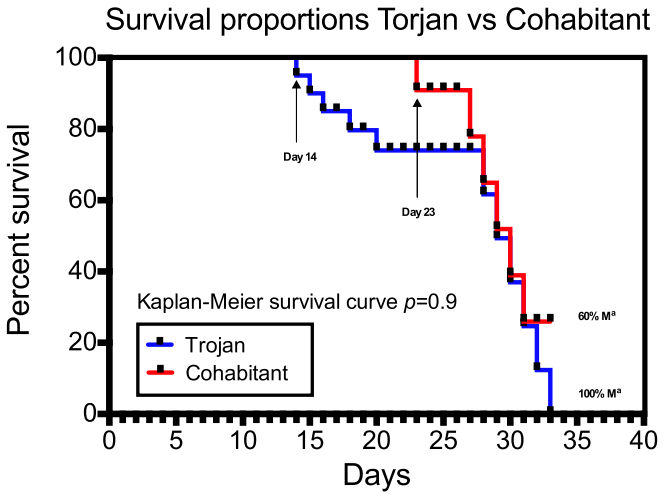

Fig. 1. Kaplan–Meier survival curves for length of time after randomization until occurrence of primary endpoint (death from ISAV-challenges) for the ip-injected fish (Trojans) and cohabitation infected fish. The number of fish experiencing the primary death is indicated. We calculated the survival fractions using the product limit (Kaplan–Meier) method. For each value (time), the figures show the fractions still alive.

kidney and gills of five moribund or dead fish were fixed in 10% buffered formalin for histopathological- and immunohistochemical (IHC) examination (data not shown).

2.4. Fish RNA extraction

From 30 mg of each tissue, total RNA was isolated using RiboPure™ Kit (Ambion, USA) according to the manufacturer's instructions. RNA concentration and purity were estimated using the NanoDrop 1000 Spectrophotometer (Thermo Scientific), while the RNA integrity number (RIN) was evaluated through the 2200 TapeStation (Agilent technologies, USA) using the R6K screen tape. Samples with RIN $\geq$8 and 260/280 ratio equal to 1.8 were used for library construction.

2.5. Library construction and Illumina sequencing

Total RNA from each time (T0, T1, T2, T3) and tissue (Gills, head-kidney and liver) were pooled, considering five randomly selected individuals per pool. From these pools, twelve barcoded libraries were constructed using the Truseq™ RNA Sample Preparation Kit v2 (Illumina, USA) according to the manufacturer's instruction. Briefly, from 1 μg of pooled total RNA, mRNA was isolated and fragmented, followed by double-stranded cDNA synthesis. Later, ends were repaired and adenylated at the 3′ end in order to perform the Illumina adapter/index ligation and final PCR amplification. Library validation was based on length distribution as estimated with the 2200 TapeStation (Agilent Technologies, USA) using D1K screen tape and reagents (Agilent Technologies, USA). Libraries with mean length peaks above 290 bp were used for sequencing and were quantified by qPCR using the Library Quantification Kit Illumina/Universal (Kappa, USA) according to the manufacturer's instructions. Two biological replicates were used for each condition, and sequencing was performed with the Miseq (Illumina) platform using a run of 2 x 250 paired-end reads at the Laboratory of Biotechnology and Aquatic Genomics, Interdisciplinary Center for Aquaculture Research (INCAR), Universidad de Concepción, Chile. The cleaned short read sequences were deposited in the Sequence Read Archive (SRA) (http://www.ncbi.nlm.nih.gov/sra) under the accession number SRX658605. The *de novo* assembly sequence data is available from corresponding author on request.

2.6. Data analysis

***De novo* assembling.** Sequencing data analysis was performed using the CLC Genomics Workbench software Version 8.0 (CLC bio, Denmark). Raw data obtained from six sequencing runs were filtered by quality and adapter/index trimmed. CLC bio's *de novo* assembly algorithm was used to create a contig list from previously filtered reads using a mismatch cost = 2, insertion cost = 3, deletion cost = 3, length fraction = 0.8, similarity fraction = 0.8, and a minimum contig length = 250. Finally, contigs were adjusted by mapped reads and end gaps where treated as mismatches. In addition, as a quality control, *de novo* assembly contigs were mapped against the last draft of the *S. salar* genome (Acc. No. AGKD00000000.3), considering a mismatch cost = 2, insertion cost = 3, deletion cost = 3, length fraction = 0,8 and a similarity fraction = 0.8. **RNA-Seq.** Different RNA-Seq analyses were performed for each sample and tissue by mapping filtered reads against the contig list obtained from *de novo* assembly. The considered parameters included a minimum read length fraction = 0.9, minimum read similarity fraction = 0.9 and unspecific read match limit = 10 in relation to the reference. Expression values were estimated as Read Per Kilobase of exon model per Million mapped reads (RPKM). ***In silico* gene expression analysis.** With the purpose of identifying highly regulated genes during ISAV infection in each tissue, the Z-test was used for statistical analysis [28]. This test is aimed to count data and compares single samples against single sample. It is based on an approximation of the binomial distribution by the normal distribution, and taking account proportions rather than raw counts, in addition p-values were FDR corrected. A Volcano plot was used to select and extract the most differentially expressed contigs, where those considered highly regulated $|\text{fold changes}| > 4$ and p-values < 0.01, as compared to the control group (T0). Similar approach has been previously described in order to develop and analyse transcriptome data through a *de novo* RNA-Seq analysis [29]. **Clustering and gene annotation.** The contigs selected using the Volcano plot were clustered according to their expression patterns and grouped in heat maps. First, normalized expression values were $\log_2$ transformed, followed by a hierarchical clustering of features. The Manhattan distance was estimated and an average linkage was selected as a clustering strategy. Contig annotations were performed based on protein similarity, thus, contigs nucleotide sequences where translated to protein sequence and blasted against non-redundant (nr) protein database (BLASTx) using a word size = 3, gap cost existence = 11, extension = 1, and a BLOSUM62 matrix.

2.7. Interactome analyses

Visualization of interactions and overlays of expression profiles was carried out using Cytoscape 2.8.2. (http://www.systemsbiology.org). The interactome network was obtained from all interactions with a FBS > 6. The interactome backbone contains 5760 nodes (protein–protein and protein-DNA interactions) and 99,573 relationships between these proteins (interactions) (Table S1). The designation of protein properties was drawn from Alexeyenko et al. 2010 [30], NCBI gene name attributes were used to unify the protein list and were imported through the Biomart plugin. The network for the immune response was built from within the Danio_rerio_CS interactome. Topological analysis of individual and combined networks was performed with Network Analyzer and jActiveModules 2.2 was used to analyse network characteristics [31,32]. GO analyses were conducted with the Biological Network Gene Ontology (BinGO, version 2.0) plugin [33] used for statistical evaluation of groups of proteins with respect to the current annotations available at the Gene Ontology Consortium (http://www.geneontology.org). GO overrepresentation was calculated using the hypergeometric test with Benjamini and Hochberg false discovery rate (FDR) multiple testing correction and significance (pFDR < 0.05). In addition we conducted a complementary analysis with ClusterMaker cytoscape plugin [34] using the MCL algorithm to search protein–protein interaction network modules derived from TAP/MAS (Tandem Affinity Purification/Mass Spectrometry). This approach clustered the network into modules based on PE Score to indicate the strength of the node association and given a fixed set of genes with high protein–protein affinity (interactome cluster nodes).

2.8. RT-qPCR validation and virus load

In order to validate gene expression values obtained by RNA-Seq analysis, RT-qPCR was conducted over 21 genes involved in immune response, oxidative stress, endoplasmic reticulum (ER) stress, endocytosis inhibition, proteasome and ribosome structure. Thus, genes selected and the specific primers used for validation are presented in Table S2. The qPCR runs were performed with StepOnePlus™ (Applied Biosystems, Life Technologies, USA) using the comparative ΔCt method. Each reaction was conducted with a

volume of 10 μL using the Maxima® SYBR Green/ROX qPCR Master Mix (Thermo Scientific, USA). The amplification conditions were as follows: 95 °C for 10 min, 40 cycles at 95 °C for 30 s, 60 °C for 30 s, and 72 °C for 30 s and each sample was measured considering biological and technical replicates for each measurement. Five putative housekeeping genes (HKG), Elongation factor 1-alpha, β-actin, GAPDH, 18s rRNA and S20 were statistically analysed by NormFinder algorithm to assess their transcriptional expression stability. Here, ELF was selected as HKG for gene normalization. In addition, pathogen load was determined for each sampled individual through the amplification of the ISAV segment 8 through Taqman RT-qPCR as described by Snow et al. 2006 [35] and a relative quantification of the remaining segments were performed as described by Valenzuela-Miranda et al. 2015 [36].

3. Results

3.1. Cohabitation challenge

To replicate the main route of infection by ISAV, cohabitation challenge was performed using a highly virulent ISAV strain (HPR7b). Pathogenicity of the selected strain was corroborated by the accumulated mortality in both trojans and cohabitants, followed by clinical and molecular confirmation of fish death as a result of ISAV infection. The first trojans that died were recorded 19 days post-challenge (DPC), and 100% accumulated mortality of trojans was recorded at 30 DPC. Meanwhile, the first mortality of a cohabitant was reported at 23 DPC, followed by gradually increasing mortalities that reached a plateau of 60.71% at 30 DPC. The higher mortality among fish used as trojans was 100%, which did not affect the tests. However, according to estimates of survival by Kaplan–Meier, these differences were not significant for the lifetime of the fish used between trojans and cohabitants (Fig. 1). Given these observations, samples were taken at the beginning of the challenge (T0), before the beginning of mortality, at 19 DPC (T1), with the beginning of mortality, at 23 DPC (T2), and 30 DPC (T3) when the plateau phase began.

Quantitative PCR (qPCR) assays targeting ISAV loads were estimated through the quantification of virus segment 8 using qPCR and Taqman probes, as described by Snow et al. (2006) [35]. QPCR assays designed to measure the ISAV HPR7b isolate specifically were performed on each fish sampled during the challenge as previously described [36]. The temporal expression of the viral load showed a slight increase of the viral load until the day 19 and follows of a potent increase of the ISAV-RNA abundance that reaches a maximum 23 days after the treatment then decrease further until the day 30 (Fig. 2). Mostly tissues collected from the mortalities in the trojans group had detectable quantities of the ISAV. Despite that fish without visible symptoms were sampled, RT-qPCR confirmed the presence of ISAV in these individuals.

3.2. Sequencing and RNA-seq de novo

Global expression profiles of each tissue screened (Gills, Liver and Head-kidney) were compared between each sampling time (T0, T1, T2, T3). The expression profile was carried out on a Miseq® Illumina sequencer with every run considering two distinct libraries constructed with RNA samples from the four sampling times. One hundred ninety three million reads passed the quality control for random effects between single-slide variability, leaving only transcripts that were either present or marginal in all RNA-seq experiments. From the filtered reads, *de novo* assembly was performed, and 196,846 contigs were generated with an N50 value equal to 1171 and with effective mapped reads of 84.66% (Table 1). As a quality control, the generated contigs were mapped against the last draft released of the *S. salar* genome (Data not shown). The 78.72% the contigs generated were effectively identified in the salmon genome. These data show a high coverage of the assembled reads, and just a 22% of sequences without significant matching to Salmon genome. In consequence, the high magnitude of the represented data may increase the knowledge of the gene regulation during ISAV infection. Contigs that were not matched were mapped to the salmon unigenes, resulting in 23.9% of contigs that matched against this database but not to the salmon genome. All these transcripts were used for statistical analysis to find mRNAs with abundance levels that significantly differed between each experimental time/tissue with the control group. The most significantly regulated genes were selected using a Volcano plot (data not shown), which resulted in the identification of 1591 contigs from the liver, 1484 contigs from the head-kidney, and 918 contigs from the gills (Table 2). BLASTx analysis was conducted for highly regulated contigs with the purpose of annotating contigs in functional proteins. An E-value of 1E-05 was used as a cut-off value to discriminate between annotated and non-annotated contigs. BLASTx results showing that 75% of the contigs were annotated while the remaining 25% were not. The species distribution of annotated sequences revealed that 45% of the annotated proteins were associated with salmonid species. Of these, *O. niloticus* and *D. rerio* accounted for 22% of the annotated proteins, while 34% from other fish species were archived (Fig. 3). Unannotated contigs were removed and the remaining sequences were manually depurated in order to discard duplicated and hypothetical proteins,

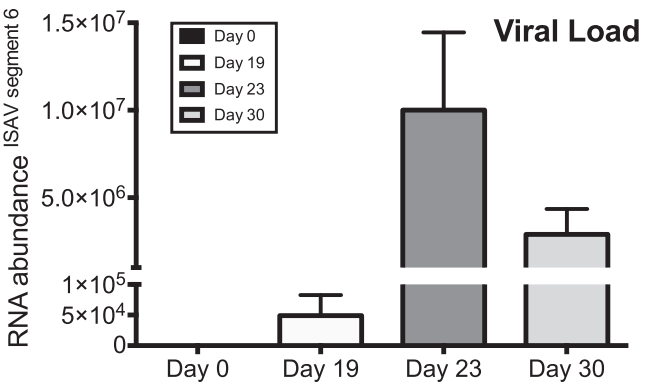

Fig. 2. Relative quantification of viral loads. Relative amount of viral load estimated in a liver and head-kidney tissue mix through RT-qPCR in five cohabitant individuals per time.

Table 1
Summary of sequencing and de novo assembly.

Sequencing	Count	After trimming
Head kidney	74.698.200	74.471.440
Liver	63.995.251	63.438.069
Gills	57.490.566	55.846.415
Total reads	196.184.017	193.755.924
de novo assembly	Without scaffold	With scaffold
N75	532	529
N50	1.171	1.138
N25	2.613	2.511
Average	834	824
Count	196.846	199.392
Mapping	Count	Percentage of reads
References	196.849	–
Mapped reads	162.037.457	84.66%
Not mapped reads	29.357.249	15.34%
Reads in pairs	104.500.498	54.60%
Broken paired reads	43.974.867	22.98%

Table 2
Distribution of annotated and not-annotated contigs among clusters and tissues.

Cluster	Liver		Head-kidney		Gills	
	Annotated	Not-annotated	Annotated	Not-annotated	Annotated	Not-annotated
1	542	174	265	150	301	100
2	143	16	95	22	96	10
3	250	80	287	84	131	25
4	303	83	439	142	167	88
Total	1238	353	1086	398	695	223
	1591		**1484**		**918**	

resulting in 337, 338 and 442 clean transcripts for gills, liver and head-kidney respectively.

3.3. Virus segment transcription

RT-qPCR was used to examine the mRNA abundance of the ISAV-segments in all tissue examined (Gills, liver and head-kidney) and time-points (T1, T2 and T3). The results obtained shows a specific transcription pattern triggered independently in each tissue (Fig. 4). Herein, Gills evidenced a significantly over-regulation of the segment S3NP in all time points (one-way ANOVA, $P < 0.05$). The segments S1PB2 and S2PB1 showed a weak increase in the time T2 and 3. In liver, the temporal expression of the ISAV segments had an inverse pattern that the observed in gills and head-kidney; Low abundance of almost all viral segment, however the segment S7NSP showed significant increase at T1 (one-way ANOVA, $P < 0.05$). The other segments showed a similar expression pattern that the observed in gills and head-kidney (Fig. 4). In contrast in head-kidney, the abundance of the viral segments registered a similar expression pattern that the observed in gills, where the segment S3NP was significantly over-regulated in all time points (one-way ANOVA, $P < 0.05$).

3.4. Gene expression analysis

Under constant housing conditions the fish in the cohabitation challenge exhibit different global profiles in the analysed tissues transcriptome. The hierarchical cluster analysis highlighted differences between the transcriptomes where gills, liver and head-kidney could easily be separated and major clusters where identified composed entirely of either tissue (Fig. S1). Analysis for mRNAs

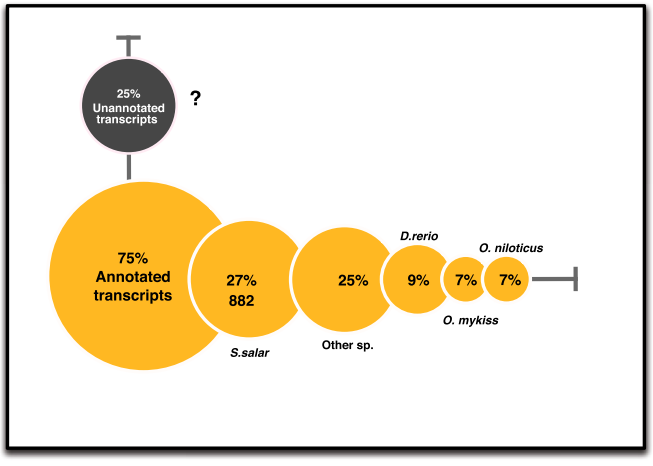

Fig. 3. Summary of annotation of differentially transcribed contigs. Percentage of unannotated and annotated contigs and species distribution of annotated genes trough blastx considering not annotated E-value > 1E-05.

that significantly differed between each time and tissue (nonparametric t-test with Benjamini and Hochberg FDR correction and $p < 0.01$) identified 337, 338 and 442 mRNAs that significantly differentiated in each tissue respectively (Fig. 5). These mRNAs are listed in the Supplementary data table with their expression levels and functional annotations (Table S3). The dendrograms show the clustering based in the gene expression pattern for each tissue. Transcripts were clustered using a hierarchical cluster algorithm, which identify four major clusters in gills and liver and five in head-kidney. Of particular note the differences on the regulation of transcripts related with key cellular processes that shown specific gene regulation between the different tissues. We observed a set of mRNAs up regulated in gills highly linked with inflammatory response. We identify a group of 337 transcripts with roles in non-specific innate immunity, inflammatory and antiviral responses such as the interferon-induced GTP-binding protein Mx, as well as other immunomodulating cytokines such as CC-chemokine 8, prostaglandins PTGS2, PTGES3. The peak expression of this group of mRNAs was relatively high and occurred in the later times point (T2, T3). Peroxiredoxin-5 mitochondrial precursor, ATP-binding cassette sub-family F member 1, Interleukins IL1R, IL1B, IL10RB, IL13RA2, IL18 and matrix metalloproteinase-9 and 1 were upper-expressed in many time-points (Table 3a). Other transcripts such as Caspase 3 and tumour necrosis factor (TNF) superfamily member 10, TRAF1, CD209 were under-expression in early points, while being over-expressed at the late time-points.

In the other hand anti-viral and interferon function was observed to a higher abundance in Liver including RIG-like receptors (RLRs) and NOD-like receptors (NLRs), DEXH (Asp-Glu-X-His) box polypeptide 58 (*lgp2*), the melanoma differentiation associated gene 5 (*mda5*), and the NLR NOD-like receptor family CARD domain containing 5 (*nlr5*) several transcription factors were activated that induced the transcription of interferon mediated immunity, such as the group of interferon regulation factors (IRF) and signal transducer and activation factors (STAT), which were also up-regulated between clusters (Table 3b). Of the up-regulated antiviral genes, it was possible to identify in all three tissues genes coding for Myxovirus resistance proteins, Gig2-like proteins, Viperin, and the VHSV-induced protein. Furthermore in the head-kidney transcript set a significant number of related mRNAs directly involved in regulation adaptive immune response and with known or putative roles in antigen presentation via MHC class II molecules or I. Beta-2-microglobuline precursor and class I histocompatibility antigen F10 alpha chain precursor, which form the MHC class I complex and present antigens to CD8+ cytotoxic T cells, were over-expressed. As well as, cell differentiation and proliferation status including: Type VII collagen Alpha 1, Procollagen-proline, Disintegrin 28, Metalloproteinase 9, Cyclin T1, Progenitor cell differentiation and proliferation factor b also were over-expressed (Table 3c). These diametrically opposed observed abundances in key immunological transcripts suggest that the underpinning regulation of antiviral, inflammatory, cellular proliferation and innate immune response may be dependent upon the

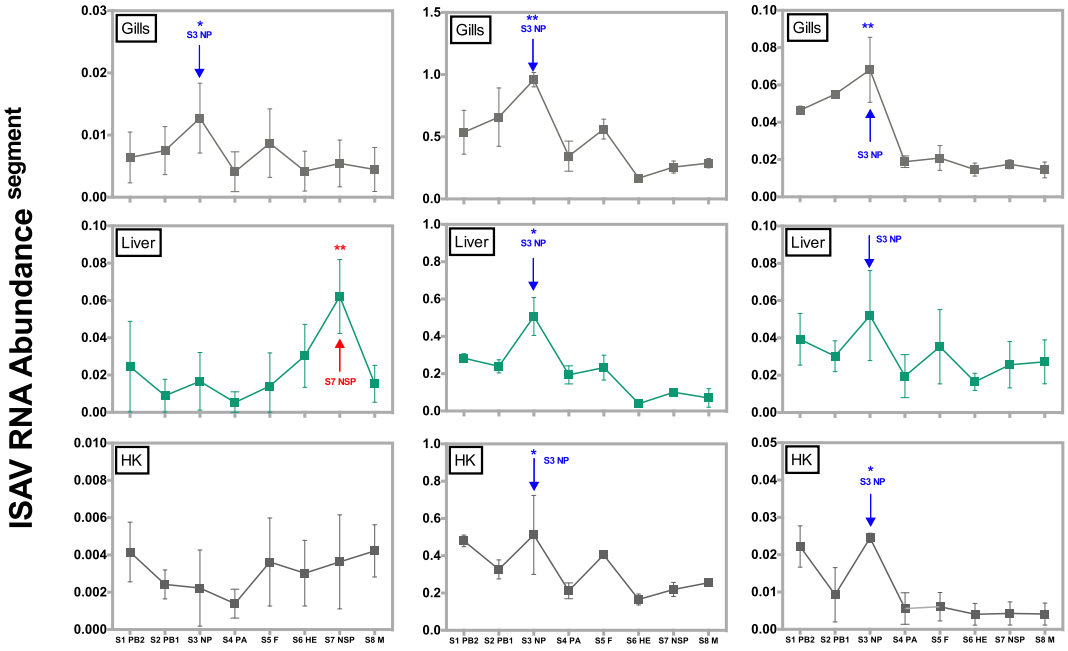

Fig. 4. Comparison of transcription values obtained all Segment (S1–S8) obtained by RT-qPCR, by each tissue (Gills, liver and head-kidney) and time points. Mean (±SE), one-way ANOVA (*p < 0.05; **p < 0.01).

tissue and reflects a tightly correlation with the viral segment transcription, in addition reveals a differential immunological status of each tissue.

3.5. ISAV-induce a tissue specific interactome and GO process

In order to further explore the functional significance of ISAV-induce a tissue-dependent differences in the transcriptome modulation, we developed a stringent analysis using selected clusters of transcripts that share a high protein–protein affinity (interactome analysis). For interactome-based analysis we used the global network of functional coupling for zebrafish and combined this data with our RNA-seq dataset to create 3 tissue-specific interactomes using the Cytoscape platform (data not shown). We identified network regions (sub-portions of the full network) enriched in differentially expressed, interconnected mRNAs (nodes) specific for gills, liver and head-kidney. We selected the modules with the highest representation of node–node interactions that were found in each tissue and conducted GO analysis with the ClueGo plugin [37]. Three distinct predicted biological outcomes were obtained (Fig. 6). As suggested and supporting our previous analysis modules with significant differences were identified in the tissues-specific interactomes. As shown in Fig. 6, the GO processes mostly regulated in gills are related with macrophage activation, cellular migration as well as activation of the innate immune response, in stark contrast that the observed in liver, where the GO over expressed were interferon and antiviral response. In head-kidney several immunological process were up-regulated and were linked with adaptive immune response, as well as, leukocyte activation, cell differentiation or immune effector process. This analysis supports the observation that ISAV directly affects key immunological processes, which are specific of tissues examined.

3.6. Expression values validated through RT-qPCR

Furthermore, to validate the novel processes that showed to be highly regulated during ISAV infection in *S. salar*, RT-qPCR were conducted over several genes. Results are presented in Supplementary Fig. 2S, Herein expression values obtained for genes regulated in liver (White plots) showed increased transcriptional values at T2 and mainly at T3, such as in genes involved in the endoplasmic reticulum stress (GRP78, HS70P4 and ERHSP40), proteasome (PSU6 and PSU7) and ribosome (RiboL5), thus supporting the results obtained by RNA-Seq. In addition, several genes in head-kidney (Dark plots) were also tested, and the results obtained were also correlated with those obtained by RNA-Seq. Thus, a down regulation at T2 of cell adhesion molecules (ITG4, Stab1 and Stab2), endocytosis gene Gi24 and proteins that mediate the attachment of cell membranes to cytoskeleton (Ankyrins) was confirmed by qPCR. In addition, to validate expression values estimated by RNA-Seq analysis, RT-qPCR was conducted over 24 genes different genes available in Table S2. Specifically, expression values from RNA-Seq and RT-qPCR were obtained for each sampled time, and a scatter graph was plotted by comparing fold changes values obtained from RNA-Seq (on the X-axis) and fold changes obtained from RT-qPCR (on the Y-axis). The correlation between both techniques is showed in Fig. 7 and the regression function is presented, showing a Pearson correlation of 0.93.

4. Discussion

Massive gene expression tools such as microarray or RNA-seq have been used to addressing viral disease in salmonids or in flatfish including; infectious salmon anaemia (ISA) [38], rhabdovirus infections including infectious hematopoietic necrosis (IHN) [39,40], viral haemorrhagic septicemia (VHS) [41,42], hirame rhabdovirus infection (HIRRV) [43] and nodavirus in the turbot [44]. With the purpose to improve the insights into the transcriptional response of Atlantic salmon to an ISAV infection, RNA-Seq analysis was conducted in the gills, liver and head-kidney of individuals infected. The use of functional genomics tools enabled us identify several immune components, which are either activated or repressed after ISAV infections. Since cohabitation has been described as the main route for ISA transmission from sick to healthy salmons [9,10], it was selected as the challenge method.

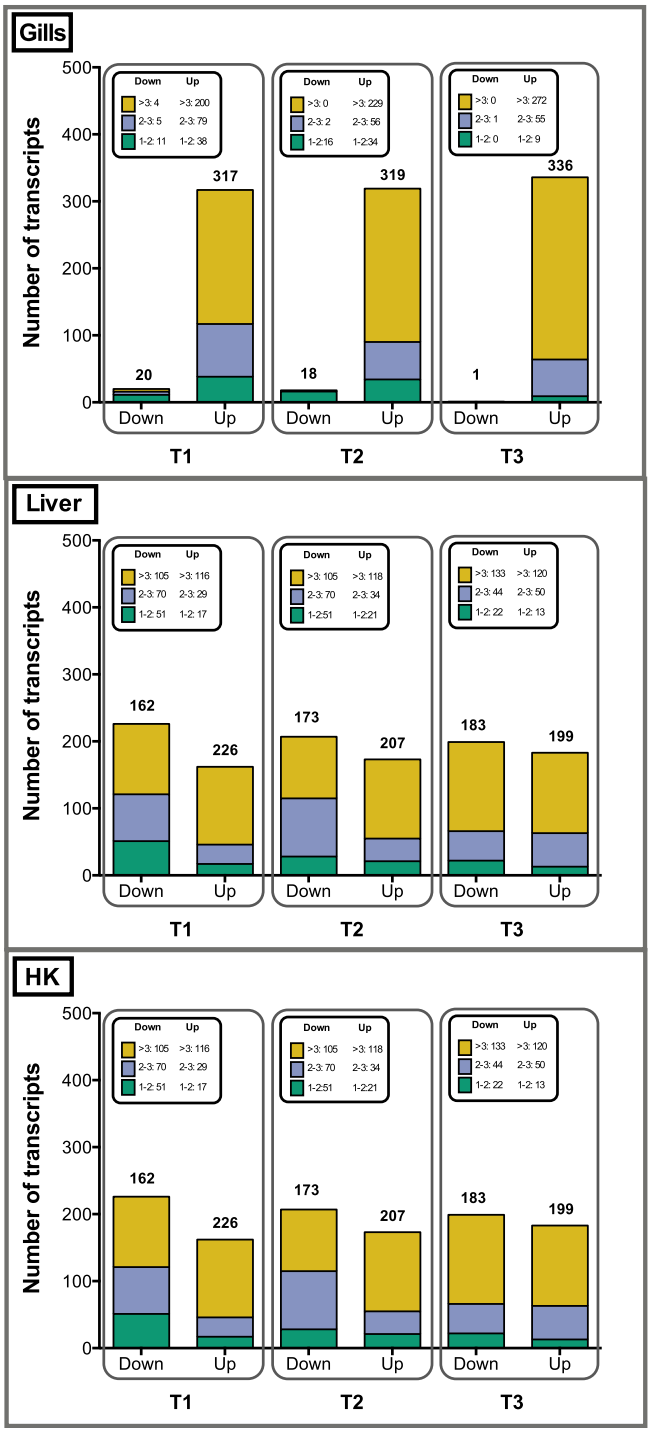

Fig. 5. Number of transcripts up/down-regulated in salmon tissues infected with ISAV. The square indicates the fold-changes values and the expression values (RPKM) for each category.

Taking into account the accumulated mortality and viral loads presented in cohabitant individuals, it was possible determined an ISA outbreak in cohabitant individuals. In contrast, fish infected by cohabitation with the same isolate than the Trojans had a cumulative mortality of 60%. Using an RT-qPCR assay to measure ISAV HPR8 viral loads in infected fish, we were able to show that the number of fish infected and the viral loads in the ip-infected were considerably higher at the various time-points than the infected by cohabitation. This increase in survival in cohabitants suggested that some sort of cross-immunity components were present. In addition this result suggests that even though cohabitants were susceptible to ISA infection, the reduced viral load and stabilized mortality could be the consequence of adaptive mechanisms to the viral infection.

Through RNA-Seq analysis, highly regulated contigs were identified in the lives, head-kidney, and gills. Our results highlight that the liver display a large number of differentially gene expressed in response to ISA infection. Similar results had been found by previous work that suggest that liver trigger a high diversity of immune related genes [20]. Annotation through BLASTx showed that from the high regulated genes 55% were annotated for different species from salmonids, thus providing a valuable source applicable to the identification of further novel transcripts for salmonid species and that are clue to the infective ISAV process. Moreover, non-annotated contigs were present within highly regulated clusters. Although these non-annotated contigs could be the result of *de novo* assembly algorithm artefacts, these groups of contigs might be involving new transcripts that had a direct relation to the infection process and host response. Due to this possibility, the complete list of non-annotated contigs, together with their fold-change transcription values for each cluster and tissue sampled were reported in the present study.

In addition we analyse the mRNA abundance of S7NP segment of ISAV, an ISAV protein with properties comparative to those of NEP of influenza viruses [45], this segment also encodes the non-structural (NS) protein of ISAV [23]. The organization of the ISAV genomic segment 7 resembles that of the corresponding segment of the influenza viruses, where the interferon (IFN) antagonist NS1 and NEP are transcribed by the collinear and spliced transcripts, respectively [46]. This feature has important consequences to that stable secondary RNA structures in the genomic segment 7 of ISAV could be involved control of viral RNA replication [45]. In our study, the ISAV S7 mRNA was found to be a gradually accumulating during the virus replication, expressed at a high level during infection in Liver in stark contrast that the pattern observed in Gills and Head-kidney, where the ISAV S3NP show higher abundance. This mechanism suggests a difference in the intracellular environment underpinning the viral replication that is highly dependent of the tissue examined. Also indicate the key importance of the NEP function in the infection cycle and thus could possibly be universal targets for interaction with key mRNA of the host defence response.

In parallel to this exciting progress the measurement of gene expression (functional genomics) has been greatly facilitated by the increasing availability of transcriptomic technologies including RNA-Seq methodologies. In this study transcriptional characterization by RNA-seq showed that the mRNAs abundance were regulated differentially among the different tissues examined. Liver displayed a gene array of mRNA highly linked with interferon and antiviral response such as the viral sensors RLRs and NLRs, described as key regulators of the antiviral defence response and confronted by a DNA or RNA viruses [47–50]. Although *RIG-I* stimulation was previously demonstrated after ISAV infection [51], to the best of our knowledge this is the first report demonstrating that *MDA5, LGP2,* and *NLRC5* were also induced in liver during ISAV infection in the Atlantic salmon. Similar results have been previously shown for *MDA5* and *LGP2* in macrophage cell lines of *Oncorhynchus mykiss* exposed to other RNA viruses [52]. In addition, several interferons related mRNAs were over-expressed in Liver. Interferons (IFN) are a key antiviral defence in vertebrates, with many well characterized IFN-induced genes expressed following their release, that participate in various ways to try to inhibit virus replication and modulate immune responses [26,53]. Interferons are usually secreted and need to interact with the

Table 3a
Subset of immune related transcripts expressed in Gills.

Description	Fold change T_0–T_1	Fold change T_0–T_2	Fold change T_0–T_3
Receptor (chemosensory) transporter protein 3	122.44	113.54	86.3
Interleukin 20 receptor, alpha	67.09	149.64	48.27
Interleukin 1, beta	4.35	5.03	2.3
Leukocyte cell-derived chemotaxin 2 precursor	−1.19	−1.52	65.93
Prostaglandin E synthase 3	1.17	1.35	4.14
Prostaglandin G/H synthase 2b	4.86	4.87	−1.27
Chemokine (C−C motif) ligand 8	3.74	4.59	2.69
TNF receptor-associated factor 1	4.22	7.01	3.66
CD209 antigen-like protein E	4.06	3.04	1.74
Tumour necrosis factor ligand superfamily member 10	2.47	3.05	4
Caspase 3	6.56	6.56	7.01
Complement component 3	1.68	2.3	138.14
Interleukin 18	5.72	1.83	1.91
Myxovirus (influenza virus) resistance 1, interferon-inducible protein	31.44	28.79	12.91
Matrix metallopeptidase 9	16.69	4.27	5.1
Mx3 protein	16.25	17.2	7.31
Gig2 (TRIB1)	4.75	6.41	3.53

Table 3b
Subset of immune related transcripts expressed in Liver.

Description	Fold change T_0–T_1	Fold change T_0–T_2	Fold change T_0–T_3
DEXH (Asp-Glu-X-His) box polypeptide 58	41.67	16.83	13.4
DEAD (Asp-Glu-Ala-Asp) box polypeptide 5	5.46	4.79	5.17
Myxovirus (influenza virus) resistance 1	16.06	33.89	10.42
NOD3	8.5	4.62	3.16
NLR family, pyrin domain containing 3	13.44	13.81	2.48
NLR family, pyrin domain containing 12	21.83	15.52	8.69
Tripartite motif-containing 25	60.46	43.27	18.91
Tripartite motif-containing 26	18.89	45.87	30.53
Tripartite motif-containing 29	17.21	23.05	7.45
Tripartite motif-containing 33	1.23	5.9	3.62
Signal transducer and activator of transcription 1	75.58	62.75	37.97
Signal transducer and activator of transcription 3	8.97	9.67	5.21
Guanylate binding protein 1, interferon-inducible	35.69	25.56	3.23
Interferon regulatory factor 1	9.76	12.56	6.18
Interferon regulatory factor 3	35.57	29.46	20.22
Interferon regulatory factor 7	19.84	19.85	16.57
Interferon regulatory factor 9	5.12	5.27	4.08
Interferon induced with helicase C	21.16	24.65	16.08
Interferon-stimulated 20 kDa exonuclease-like 2	2.08	2.21	5.93
Gig2 (TRIB1)	3.04	3.54	4.38

Table 3c
Subset of immune related transcripts expressed in Head-kidney.

Description	Fold change T_0–T_1	Fold change T_0–T_2	Fold change T_0–T_3
Immunoglobulin IghMV VH4 region	8.19	45.15	17.54
Immunoglobulin lambda polypeptide 1 precursor.	1.38	4.34	1.53
immunoglobulin lambda polypeptide 5	1.35	9.29	4.33
HLA-B	8.06	2.46	3.94
HLA-A	1.59	4.72	3.76
HLA-C	2.85	65.51	1.36
major histocompatibility complex class I related gene protein like	3.85	7.77	3.88
Metalloproteinase inhibitor 2	−5.04	−10.96	3.45
Matrix metalloproteinase-9	2.77	4.98	4.13
Progenitor cell differentiation and proliferation factor b	2.62	5.23	3.83
B cell receptor CD22	2.22	4.67	6.4
H 2 class II histocompatibility antigen gamma chain	−1.06	1.23	5.46
CD83	4.26	3.73	2.79
Granulocyte colony-stimulating factor receptor precursor	3.43	16.82	4.52
c Fos protein	25.65	1.64	3.59
Interferon-induced guanylate-binding protein 1	5.92	5.64	3.84
leukocyte receptor cluster member 8	2.26	6.71	5.29
Cyclin L1	−1.97	4.38	2.42
Disintegrin and metalloproteinase domain-containing protein 28	−2.04	4.02	3.16
macrophage mannose receptor 1	8.37	8.18	10.4
Progenitor cell differentiation and proliferation factor b	1.78	4.47	3.65
Myxovirus (influenza virus) resistance 1, interferon-inducible protein	40.5	39.54	5.33
T cell immunoglobulin and mucin domain containing protein 4 like 2	7.01	12.43	7.27
Gig2 (TRIB1)	2.96	19.03	6.71

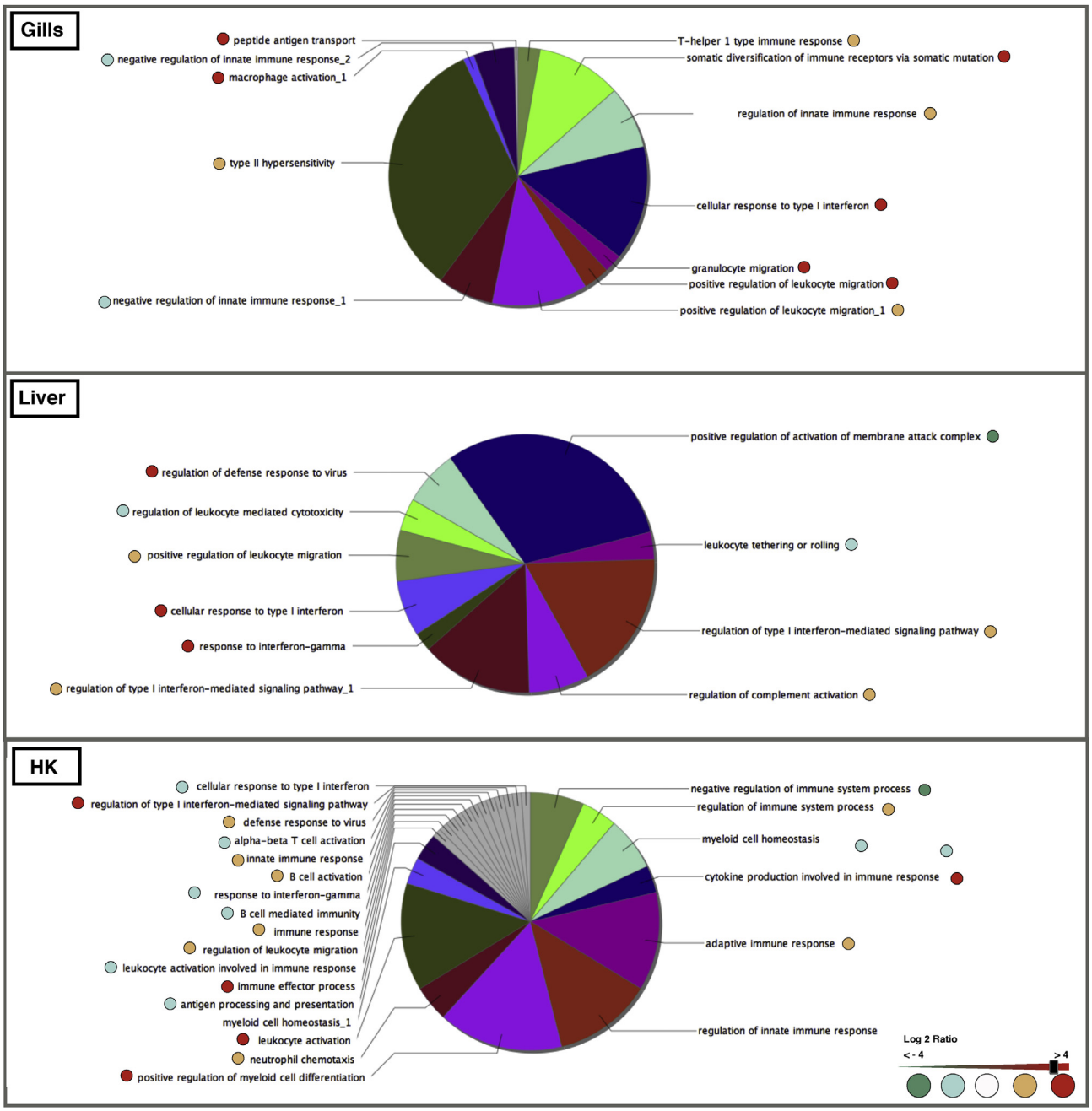

Fig. 6. Interactome mapping of tissue-related gene networks in the A. salmon Interactome modules of mRNAs expressed in each tissue based in MCL algorithm (ClusterMaker plugin) The symbols represent specific GO processes. (B) Gene ontology analysis (BinGO plugin) of each interactome-module of overexpressed GO categories ($P < 0.01$), the colour scale bar indicates relative abundance (high-low) of GO categories in each biological process. Sample size, n = 398 in Gills, n = 121 in Liver, n = 110 in HK. (For interpretation of the references to colour in this figure legend, the reader is referred to the web version of this article.)

receptors on the cell surface to initiate intracellular responses. Chang et al., 2013 [54], have demonstrated that in vitro studies with RTG-2 cells that the IFNs can also function intracellularly in trout. They found that MDA5, RIG-I or LGP2 that detect intracellular virus were upregulated by the intracellular interferon (iIFN), as well as Mx1, Stat1 and Stat2. Inquisitively, in our study were observed diverse mRNAs overexpressed and triggered by ISAV and tightly linked with the iIFN-pathway. During the virus infection, IFNs could be stored in the cytoplasm of infected cells and released in relatively large amounts should the cells be killed, alerting neighbouring cells through their surface receptors [53–55]. In this way, iIFNs may be acting as effector molecules to trigger an antiviral response following virus infection, perhaps avoiding some of the many ways in which viruses can disrupt these pathways [54,55]. The transcriptional performance shows that ISAV-induce several iIFNs-related mRNAs in liver in contrast that the observed in other tissues examined. However, to check this hypothesis ISAV-infected Atlantic salmon, further investigations are required.

In addition to innate immune-related genes, it was also possible to identify an upregulation of the adaptive immune response in Gills and head-kidney. One of the remarkable processes upregulated during ISAV infection was that involving protein processing in the ER, which was found mainly in the liver and was particularly related to ERAD and the UPR. Both mechanism are triggered as a

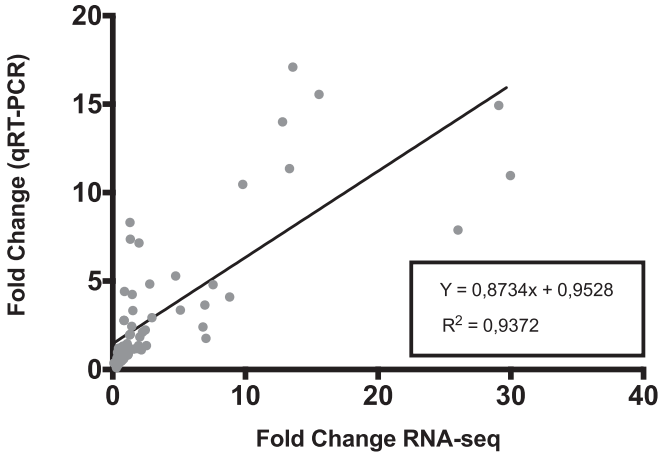

Fig. 7. RT-qPCR validation of fold change values obtained by RNA-Seq. Scatter plot of fold change values obtained from RNA-Seq (X-axis) and RT-qPCR (Y-axis) from 21 different genes.

result of misfolded proteins accumulation during ER stress caused by adverse environmental conditions, including pathogen infection [56]. Although ER stress has been studied as a stress and homeostatic mechanism [57], recent evidence suggests that it might be involved in viral pathogenicity. For instance, the influenza A virus, which belongs to the *Orthomyxoviridae* family, has been shown to induce ER stress through the IRE1 pathway [58,59]. Moreover, the inhibition of IRE1 activity has been shown to deplete viral replication, and has since become a candidate gene for a therapeutic target of the influenza A virus in humans [59]. In fish, it has been also shown that viral infections could lead to ER stress [60,61]. The results highlight that the liver trigger a suite of genes linked with antiviral response, B lymphocyte differentiation and maturation and activation of T lymphocyte-mediated immunity including CD9, CD40 and IFNg provides strong evidence for the coordinated regulation of the two arms of the piscine immune system in response to ISAV infection. In addition these diametrically opposed gene expression pattern suggest that the underpinning regulation of antiviral, inflammatory, cellular proliferation and innate immune response is dependent upon the tissue examined.

Gene expression is a complex trait that is highly influenced by several factors such as, immunological status, by environmental factors or also demanding activities such as growth and reproduction [62–64]. Relating meaningful transcriptional changes at the level of the transcriptome requires the identification processes that have a functional significance for the individuals. This remains a major objective toward understanding the complex interactions between environmental demand and an individual capacity to respond to such demand [65]. In this study through a RNA-Seq we have shown that there are significant differences in mRNA abundance related to the function, as described by interacting gene modules e. g interferon pathway, adaptive/innate immune response and cellular proliferation/differentiation, and regulation in distinct tissues during an ISAV infection, where specific functions are controlled within the each tissue independently and a portion of the observed mRNA regulation could be highly dependent of the ISAV-segment transcription. Importantly this is the first time that strong correlations between functional modules containing significant immune process with protein–protein affinities and viral-segment transcription have been made between different tissues of ISAV-infected fish.

Our data supported at different levels of gene expression analysis suggests that the inclusion of viral-segment replication to a molecular analysis has the potential to identify important host–pathogens interactions, which are likely highly relevant toward understanding the underpinning molecular framework of immune defense response during viral infection. Such relationships cannot be identified by screening the mRNA abundance of key transcripts during immune challenges. To this is needed a complex system approach in order to integrate more information to get a coherent context to provide a map toward understanding the underlying complexity of the defence response during pathogen infections.

Acknowledgements

This study was funded by FONDAP project 1510027 (CONICYT-Chile). The fish and challenge test used in this work were funded by a CORFO INNOVA grant (09-MCSS6682). The authors thank Aquainnovo for providing the samples and for their disposition in contributing to this study.

Appendix A. Supplementary data

Supplementary data related to this article can be found at http://dx.doi.org/10.1016/j.fsi.2015.04.003.

References

[1] S.C. Clouthier, T. Rector, N.E.C. Brown, E.D. Anderson, Genomic organization of infectious salmon anaemia virus, J. Gen. Virol. 83 (2002) 421–428.
[2] E. Merour, M. LeBerre, A. Lamoureux, J. Bernard, M. Bremont, S. Biacchesi, Completion of the full-length genome sequence of the infectious salmon anemia virus, an aquatic orthomyxovirus-like, and characterization of mAbs, J. Gen. Virol. 92 (2011) 528–533.
[3] S. Mjaaland, E. Rimstad, K. Falk, B.H. Dannevig, Genomic characterization of the virus causing infectious salmon anemia in Atlantic salmon (*Salmo salar* L.): an orthomyxo-like virus in a teleost, J. Virol. 71 (1997) 7681–7686.
[4] H.M. Rowley, S.J. Campbell, W.L. Curran, T. Turnbull, D.G. Bryson, Isolation of infectious salmon anaemia virus (ISAV) from Scottish farmed Atlantic salmon, *Salmo salar* L, J. Fish Dis. 22 (1999) 483–487.
[5] D.A. Bouchard, K. Brockway, C. Giray, W. Keleher, P.L. Merrill, First report of infectious Salmon anemia (ISA) in the United States, Bull. Eur. Assoc. Fish Pathol. 21 (2001) 86–88.
[6] J.E. Lovely, B.H. Dannevig, K. Falk, L. Hutchin, A.M. MacKinnon, K.J. Melville, et al., First identification of infectious salmon anaemia virus in North America with haemorrhagic kidney syndrome, Dis. Aquat. Org. 35 (1999) 145–148.
[7] M.G. Godoy, A. Aedo, M.J.T. Kibenge, D.B. Groman, C.V. Yason, H. Grothusen, et al., First detection, isolation and molecular characterization of infectious salmon anaemia virus associated with clinical disease in farmed Atlantic salmon (*Salmo salar*) in Chile, BMC Vet. Res. (2008) 4.
[8] K. Thorud, H.O. Djupvik, Infectious anaemia in Atlantic salmon (*Salmo salar* L.), Bull. Eur. Assoc. Fish Pathol. 8 (1988) 109–111.
[9] T.M. Lyngstad, P.A. Jansen, H. Sindre, C.M. Jonassen, M.J. Hjortaas, S. Johnsen, et al., Epidemiological investigation of infectious salmon anaemia (ISA) outbreaks in Norway 2003–2005, Prev. Vet. Med. 84 (2008) 213–227.
[10] S.R.M. Jones, D.B. Groman, Cohabitation transmission of infectious salmon anemia virus among freshwater-reared Atlantic salmon, J. Aquat. Animal Health 13 (2001) 340–346.
[11] A.B. Mikalsen, A. Teig, A.L. Helleman, S. Mjaaland, E. Rimstad, Detection of infectious salmon anaemia virus (ISAV) by RT-PCR after cohabitant exposure in Atlantic salmon *Salmo salar*, Dis. Aquat. Org. 47 (2001) 175–181.
[12] S.C. Weli, M. Aamelfot, O.B. Dale, E.O. Koppang, K. Falk, Infectious salmon anaemia virus infection of Atlantic salmon gill epithelial cells, Virol. J. 10 (2013).
[13] O. Evensen, K.E. Thorud, Y.A. Olsen, A morphological-study of the gross and light microscopic lesions of infectious-anemia in Atlantic Salmon (Salmo-Salar), Res. Vet. Sci. 51 (1991) 215–222.
[14] L. Speilberg, O. Evensen, B.H. Dannevig, A sequential study of the light and electron-microscopic liver-lesions of infectious-anemia in Atlantic Salmon (Salmo-Salar L), Vet. Pathol. 32 (1995) 466–478.
[15] E. Simko, L.L. Brown, A.M. MacKinnon, P.J. Byrne, V.E. Ostland, H.W. Ferguson, Experimental infection of Atlantic salmon, *Salmo salar* L., with infectious salmon anaemia virus: a histopathological study, J. Fish Dis. 23 (2000) 27–32.
[16] I. Jensen, B. Robertsen, Effect of double-stranded RNA and interferon on the antiviral activity of Atlantic salmon cells against infectious salmon anemia virus and infectious pancreatic necrosis virus, Fish Shellfish Immunol. 13 (2002) 221–241.
[17] O. Kileng, M.I. Brundtland, B. Robertsen, Infectious salmon anemia virus is a powerful inducer of key genes of the type I interferon system of Atlantic

salmon, but is not inhibited by interferon, Fish Shellfish Immunol. 23 (2007) 378–389.
[18] B.L. Schiotz, S.M. Jorgensen, C. Rexroad, T. Gjoen, A. Krasnov, Transcriptomic analysis of responses to infectious salmon anemia virus infection in macrophage-like cells, Virus Res. 136 (2008) 65–74.
[19] S.T. Workenhe, T.S. Hori, M.L. Rise, M.J.T. Kibenge, F.S.B. Kibenge, Infectious salmon anaemia virus (ISAV) isolates induce distinct gene expression responses in the Atlantic salmon (*Salmo salar*) macrophage/dendritic-like cell line TO, assessed using genomic techniques, Mol. Immunol. 46 (2009) 2955–2974.
[20] S.M. Jorgensen, S. Afanasyev, A. Krasnov, Gene expression analyses in Atlantic salmon challenged with infectious salmon anemia virus reveal differences between individuals with early, intermediate and late mortality, BMC Genomics 9 (2008).
[21] S.M. Jorgensen, D.L. Hetland, C.M. Press, U. Grimholt, T. Gjoen, Effect of early infectious salmon anaemia virus (ISAV) infection on expression of MHC pathway genes and type I and II interferon in Atlantic salmon (*Salmo salar* L.) tissues, Fish Shellfish Immunol. 23 (2007) 576–588.
[22] F. LeBlanc, M. Laflamme, N. Gagne, Genetic markers of the immune response of Atlantic salmon (*Salmo salar*) to infectious salmon anemia virus (ISAV), Fish Shellfish Immunol. 29 (2010) 217–232.
[23] E. Garcia-Rosado, T. Markussen, O. Kileng, E.S. Baekkevold, B. Robertsen, S. Mjaaland, et al., Molecular and functional characterization of two infectious salmon anaemia virus (ISAV) proteins with type I interferon antagonizing activity, Virus Res. 133 (2008) 228–238.
[24] A.J.A. McBeath, B. Collet, R. Paley, S. Duraffour, V. Aspehaug, E. Biering, et al., Identification of an interferon antagonist protein encoded by segment 7 of infectious salmon anaemia virus, Virus Res. 115 (2006) 176–184.
[25] T. Sandvik, E. Rimstad, S. Mjaaland, The viral RNA 3'- and 5'-end structure and mRNA transcription of infectious salmon anaemia virus resemble those of influenza viruses, Arch. Virol. 145 (2000) 1659–1669.
[26] R.G. Brinson, A.L. Szakal, J.P. Marino, Structural characterization of the viral and cRNA Panhandle Motifs from the infectious Salmon anemia virus, J. Virol. 85 (2011) 13398–13408.
[27] M. Godoy, M. Kibenge, R. Suarez, E. Lazo, A. Heisinger, J. Aguinaga, et al., Infectious salmon anaemia virus (ISAV) in Chilean Atlantic salmon (*Salmo salar*) aquaculture: emergence of low pathogenic ISAV-HPR0 and re-emergence of virulent ISAV-HPRΔ: HPR3 and HPR14, Virol. J. 10 (2013) 344.
[28] A.J. Kal, A.J. van Zonneveld, V. Benes, M. van den Berg, M.G. Koerkamp, K. Albermann, et al., Dynamics of gene expression revealed by comparison of serial analysis of gene expression transcript profiles from yeast grown on two different carbon sources, Mol. Biol. Cell 10 (1999) 1859–1872.
[29] C. Gallardo-Escarate, V. Valenzuela-Munoz, G. Nunez-Acuna, RNA-seq analysis using de novo transcriptome assembly as a reference for the Salmon Louse Caligus rogercresseyi, PLoS One 9 (2014).
[30] A. Alexeyenko, D.M. Wassenberg, E.K. Lobenhofer, J. Yen, E. Linney, E.L.L. Sonnhammer, et al., Dynamic zebrafish interactome reveals transcriptional mechanisms of dioxin toxicity, PLoS One 5 (2010).
[31] J. Montojo, K. Zuberi, H. Rodriguez, F. Kazi, G. Wright, S.L. Donaldson, et al., GeneMANIA Cytoscape plugin: fast gene function predictions on the desktop, Bioinformatics 26 (2010) 2927–2928.
[32] M.E. Smoot, K. Ono, J. Ruscheinski, P.L. Wang, T. Ideker, Cytoscape 2.8: new features for data integration and network visualization, Bioinformatics 27 (2011) 431–432.
[33] S. Maere, K. Heymans, M. Kuiper, BiNGO: a cytoscape plugin to assess overrepresentation of gene ontology categories in biological networks, Bioinformatics 21 (2005) 3448–3449.
[34] J.H. Morris, L. Apeltsin, A.M. Newman, J. Baumbach, T. Wittkop, G. Su, et al., Clustermaker: a multi-algorithm clustering plugin for Cytoscape, BMC Bioinform. 12 (2011).
[35] M. Snow, P. McKay, A. McBeath, J. Black, F. Doig, R. Kerr, et al., Development, application and validation of a Taqman real-time RT-PCR assay for the detection of infectious salmon anaemia virus (ISAV) in Atlantic salmon (*Salmo salar*), Dev. Biol. 126 (2006) 133–145.
[36] D. Valenzuela-Miranda, M.E. Cabrejos, J.M. Yañez, C. Gallardo-Escárate, From the viral perspective: Infectious salmon anemia virus (ISAV) transcriptome during the infective process in Atlantic salmon (*Salmo salar*), Mar. Genomics 20 (2015) 39–43.
[37] G. Bindea, B. Mlecnik, H. Hackl, P. Charoentong, M. Tosolini, A. Kirilovsky, et al., ClueGO: a cytoscape plug-in to decipher functionally grouped gene ontology and pathway annotation networks, Bioinformatics 25 (2009) 1091–1093.
[38] S.M. Jorgensen, S. Afanasyev, A. Krasnov, Gene expression analyses in Atlantic salmon challenged with infectious salmon anemia virus reveal differences between individuals with early, intermediate and late mortality, BMC Genomics 9 (2008) 179.
[39] S. MacKenzie, J.C. Balasch, B. Novoa, L. Ribas, N. Roher, A. Krasnov, et al., Comparative analysis of the acute response of the trout, *O. mykiss*, head kidney to in vivo challenge with virulent and attenuated infectious hematopoietic necrosis virus and LPS-induced inflammation, BMC Genomics 9 (2008) 141.
[40] M.K. Purcell, I.S. Marjara, W. Batts, G. Kurath, J.D. Hansen, Transcriptome analysis of rainbow trout infected with high and low virulence strains of infectious hematopoietic necrosis virus, Fish Shellfish Immunol. 30 (2011) 84–93.
[41] J.Y. Byon, T. Ohira, I. Hirono, T. Aoki, Use of a cDNA microarray to study immunity against viral hemorrhagic septicemia (VHS) in Japanese flounder (*Paralichthys olivaceus*) following DNA vaccination, Fish Shellfish Immunol. 18 (2005) 135–147.
[42] J.Y. Byon, T. Ohira, I. Hirono, T. Aoki, Comparative immune responses in Japanese flounder, *Paralichthys olivaceus* after vaccination with viral hemorrhagic septicemia virus (VHSV) recombinant glycoprotein and DNA vaccine using a microarray analysis, Vaccine 24 (2006) 921–930.
[43] M. Yasuike, H. Kondo, I. Hirono, T. Aoki, Difference in Japanese flounder, *Paralichthys olivaceus* gene expression profile following hirame rhabdovirus (HIRRV) G and N protein DNA vaccination, Fish Shellfish Immunol 23 (3) (2007) 531–541.
[44] K.C. Park, J.A. Osborne, A. Montes, S. Dios, A.H. Nerland, B. Novoa, et al., Immunological responses of turbot (Psetta maxima) to nodavirus infection or polyriboinosinic polyribocytidylic acid (pIC) stimulation, using expressed sequence tags (ESTs) analysis and cDNA microarrays, Fish Shellfish Immunol. 26 (2009) 91–108.
[45] R.B. Ramly, C.M. Olsen, S. Braaen, E. Rimstad, Infectious salmon anaemia virus nuclear export protein is encoded by a spliced gene product of genomic segment 7, Virus Res. 177 (2013) 1–10.
[46] R.B. Ramly, C.M. Olsen, S. Braaen, E.F. Hansen, E. Rimstad, Transcriptional regulation of gene expression of infectious salmon anaemia virus segment 7, Virus Res. 190 (2014) 69–74.
[47] M. Yoneyama, T. Fujita, Function of RIG-I-like receptors in antiviral innate immunity, J. Biol. Chem. 282 (2007) 15315–15318.
[48] M. Yoneyama, T. Fujita, RNA recognition and signal transduction by RIG-I-like receptors, Immunol. Rev. 227 (2009) 54–65.
[49] M. Schlee, Master sensors of pathogenic RNA – RIG-I like receptors, Immunobiology 218 (2013) 1322–1335.
[50] T.D. Kanneganti, M. Lamkanfi, G. Nunez, Intracellular NOD-like receptors in host defense and disease, Immunity 27 (2007) 549–559.
[51] A. Lauscher, B. Krossoy, P. Frost, S. Grove, M. Konig, J. Bohlin, et al., Immune responses in Atlantic salmon (*Salmo salar*) following protective vaccination against infectious salmon anemia (ISA) and subsequent ISA virus infection, Vaccine 29 (2011) 6392–6401.
[52] M.X. Chang, B. Collet, P. Nie, K. Lester, S. Campbell, C.J. Secombes, et al., Expression and functional characterization of the RIG-I-Like receptors MDA5 and LGP2 in rainbow Trout (*Oncorhynchus mykiss*), J Virol. 85 (2011) 8403–8412.
[53] S.A.M. Martin, J.B. Taggart, P. Seear, J.E. Bron, R. Talbot, A.J. Teale, et al., Interferon type I and type II responses in an Atlantic salmon (*Salmo salar*) SHK-1 cell line by the salmon TRAITS/SGP microarray, Physiol. Genomics 32 (2007) 33–44.
[54] M.X. Chang, J. Zou, P. Nie, B. Huang, Z.L. Yu, B. Collet, et al., Intracellular interferons in fish: a unique means to combat viral infection, PLoS Pathog. 9 (2013).
[55] K.E. Taylor, K.L. Mossman, Recent advances in understanding viral evasion of type I interferon, Immunology 138 (2013) 190–197.
[56] D.J. Todd, A.H. Lee, L.H. Glimcher, The endoplasmic reticulum stress response in immunity and autoimmunity, Nat. Rev. Immunol. 8 (2008) 663–674.
[57] P. Walter, D. Ron, The unfolded protein response: from stress pathway to homeostatic regulation, Science 334 (2011) 1081–1086.
[58] E.C. Roberson, J.E. Tully, A.S. Guala, J.N. Reiss, K.E. Godburn, D.A. Pociask, et al., Influenza induces endoplasmic reticulum stress, caspase-12-dependent apoptosis, and c-Jun n-terminal kinase-mediated transforming growth factor-beta release in lung epithelial cells, Am. J. Respir. Cell Mol. Biol. 46 (2012) 573–581.
[59] I.H. Hassan, M.S. Zhang, L.S. Powers, J.Q. Shao, J. Baltrusaitis, D.T. Rutkowski, et al., Influenza a viral replication is blocked by inhibition of the inositol-requiring enzyme 1 (IRE1) stress pathway, J. Biol. Chem. 287 (2012) 4679–4689.
[60] H.L. Huang, J.L. Wu, M.H.C. Chen, J.R. Hong, Aquatic birnavirus-induced ER stress-mediated death signaling contribute to downregulation of Bcl-2 family proteins in Salmon embryo cells, PLoS One 6 (2011).
[61] M.W. Lu, F.H. Ngou, Y.M. Chao, Y.S. Lai, N.Y. Chen, F.Y. Lee, et al., Transcriptome characterization and gene expression of Epinephelus spp in endoplasmic reticulum stress-related pathway during betanodavirus infection in vitro, BMC Genomics 13 (2012).
[62] B.C. Sheldon, S. Verhulst, Ecological immunology: costly parasite defences and trade-offs in evolutionary ecology, Trends Ecol. Evol. 11 (1996) 317–321.
[63] K. Norris, M.R. Evans, Ecological immunology: life history trade-offs and immune defense in birds, Behav. Ecol. 11 (2000) 19–26.
[64] M. Zuk, A.M. Stoehr, Immune defense and host life history, Am. Nat. 160 (2002) S9–S22.
[65] A. Whitehead, D.L. Crawford, Neutral and adaptive variation in gene expression, P. Natl. Acad. Sci. U. S. A 103 (2006) 5425–5430.